

# Heterostructure Composite of RGO/PANI/Ag as benign Photocatalyst for Paracetamol Degradation

S. Sravya<sup>1</sup>, Dharmasoth Rama Devi<sup>2</sup>, B. Sathish Mohan<sup>3</sup>, K. Basavaiah<sup>1\*</sup>

<sup>1</sup>Department of Chemistry, Andhra University, Visakhapatnam-530003, India

<sup>2</sup>Dr. Samuel George Institute of Pharmaceutical Sciences, Markapur, A.P.-523316, India

<sup>3</sup>Bio Enviro Chemical Solutions, Visakhapatnam-530017, India

## Abstract

The paracetamol waste accumulation in sewage water is increasing and becoming major concern. There are many mechanical and chemical processes to decrease the problem, photolytic degradation is one among them. Photolytic degradation is on-site process which is eco-friendly and with high impact. Graphene based nanocomposites are highly used for photo catalytic degradation, RGO/PANI/Ag nanocomposite plays a prominent role. In present case, the authors report a facile route to fabrication of RGO/PANI/Ag composite with support of reducing agent (Vitamin-C). The morphological, structural, optical, and photocatalytic properties of prepared RGO/PANI/Ag composite, obtained from sophisticated instruments (UV-Visible spectroscopy, FTIR spectroscopy, powder XRD, SEM and TEM). The results revealed the successfully formation of RGO/PANI/Ag nanocomposite. The PANI was properly diffused between RGO, it appears like porous membrane on RGO and fine crystals of Ag NPs were amalgamated. RGO/PANI/Ag nanocomposite exhibits exceptional paracetamol degradation by visible light illumination, with degradation efficiencies reaching 99.6% and 75.76% in acidic and basic media, respectively. This remarkable enhancement in degradation is attributed to the synergistic interplay within the nanocomposites.

**Keywords:** RGO/PANI/Ag nanocomposites; Paracetamol; Photocatalytic degradation

## Full-length article

\*Corresponding Author, e-mail: [klbasu@gmail.com](mailto:klbasu@gmail.com)

## 1. Introduction

Pharmaceutical contamination has emerged as a significant environmental concern over the past decade. Even trace levels of pharmaceuticals in water can have profound impacts on human health, wildlife, and aquatic ecosystems. Municipal contaminated water, hospital effluents, and industrial discharges are the primary routes of pharmaceutical contamination from its source. Among pharmaceuticals, paracetamol (4-hydroxyacetanilide) stands out mostly used analgesics and antipyretics globally [1-3]. Paracetamol's propensity to accumulate in aquatic environments poses severe concern on living organisms [4-9]. Hence, paracetamol removal from its contamination is of paramount importance.

Numerous methods previously reported to paracetamol removal from its pollution including RO, AOPs, filtration, treatment and activate sludge [10-11]. Among these advanced oxidation process i.e. photo catalysis have received more awareness as its cost less, safer and no secondary pollutant [12]. In the recent years, nanocomposites based on Graphene based materials have broader applications in optical electronics, sensors, super capacitors, catalysis, Hydrogen production and storage owing to its superior mechanical, thermal, optical and electrical properties and huge clearness, elasticity and great surface

area [12-13]. More recently, especially, nanocomposites based on Graphene and conducting polymers have emerged potential materials, due to their optical, electrical, electrochemical and mechanical properties. GO is converted to RGO and doped many materials in past which have vast advances in electrical, electrochemical and mechanical applications.

Among condensation polymers, polyaniline (PANI) and PANI based derivatives have emerged as potential material for various technological applications [28-30]. The properties of conducting polymers, such as polyaniline (PANI), are significantly influenced by various factors. PANI synthesized through the polymerization approach (chemical oxidative). This process involves the oxidation of leucoemeraldine, a partially oxidized form of PANI, to emeraldine salt, a fully oxidized and conducting form of PANI. The mechanism of protonation and deprotonation of PANI helps in catalytic degradation of Paracetamol [14]. Silver nanoparticles (Ag NPs) are prepared by using Vitamin - C as good reducing agent. Ag NPs has good dimension stability and chemically stable in acidic and basic medium, hence it is a good catalyst and eliminates micro-organisms. They help in fast degradation of carboxylic acids to carbonates and CO<sub>2</sub>. It has a good oxidation potential which favours the degradation of paracetamol [15].

RGO/PANI/Ag (one pot synthesis) compound causes good degradation of paracetamol. PANI is good conducting polymer. The Amines and Imine groups in acidic medium transfers  $H^+$  ions which accelerates the degradation, this will be further accelerated and controlled by RGO and Silver nanoparticles. Here in, we propose the fabrication of RGO supports PANI/Ag nanocomposite towards the paracetamol deprivation under visible light irradiation, also studied their degradation rate effect with various factors changing.

## 2. Methodologies

Without additional purification, Merck, India supplied the hydrochloric acid, Graphite flakes, potassium permanganate, sodium nitrate, hydrogen peroxide, sulphuric acid, Acetone, sodium hydroxide, Silver nitrate, Aniline, Ammonium per Sulphate, Hydrazine, ammonia solution, and ascorbic acid (Vitamin C) needed for the synthesis. The entire synthesis procedure was carried out with deionized water.

### 2.1. RGO/PANI/Ag composite preparation

Initially, the desirable GO was obtained from modified hummer approach [16]. GO (100 mg) was taken in RB flask of 250 mL which contains 100mL deionised water (1mg/1mL) under ultra sonication. Aniline (1M) and APS with HCl (1M) were added and allowed it under  $N_2$  at 80 °C for an hour with continuous stirring. 5mL of vitamin-C (2M) was mixed with above mixture, and ammonia solution (25%) was added after 30 min. Let the reaction continues for 2.5h at 80 °C under constant stirring. At last, the coloured precipitate with blackish green was achieved and the same was filtered, washed and dried under vacuum at room temperature for further usage.

### 2.2. Characterization

The Shimadzu 2450 instrument was employed to record the UV-Vis spectra. The X-ray diffraction (XRD) patterns were recorded using a PANalyticalX'pert pro diffractometer with  $Cu-K\alpha$  radiation (1.5406 Å, 45 kV, 40 mA) and  $2\theta$  ranging from  $10^\circ$  to  $90^\circ$  at a scan rate of 0.02  $^\circ/s$ . The powder samples were carefully mixed with KBr and shaped into thin pellets to prepare them for Fourier transform-infrared (FTIR) spectra investigation. The measuring range used to record the data was 400–4000  $cm^{-1}$ . At an accelerating voltage of 200 kV, images from transmission electron microscopy were captured (TEM from JEOL, Japan). JEOL SEM was used in this study for morphology.

### 2.3. Photocatalytic deprivation of paracetamol using nanocomposite

50 mL of the medication solution contained 50mg of prepared nanocomposite dipped in it. For catalytic degradation, the sample was first shaken in the dark for five minutes before being exposed to regular light. At the designated reaction time, the samples from the flask were removed until the adsorption equilibrium was reached. Following centrifugation of the material, the clear solution containing the remaining drug concentration was measured using spectrometer (UV-Vis with 200-800 nm range). The absorbance peak of paracetamol at 245 nm was seen to track the reactions in acidic, basic, and neutral media containing

varying ratios of paracetamol to nanocomposites in 1:1 mg/mL, 0.5:1 mg/mL & 1:0.5 mg/mL respectively. The paracetamol degradation rate (D%) was obtained from The percentage of paracetamol degradation was calculated by  $D\% = (A_0 - A_t)/A_0 \times 100$

Where ' $A_0$ ' is the initial paracetamol absorbance, ' $A_t$ ' is paracetamol absorbance in a solution at time t later than degradation.

## 3. Results and Discussion

### a. Characterization assay results

Figure 1 shows the UV-Vis bands of PANI, RGO, Ag and nanocomposite. The respective peaks were noted for RGO is at 260 nm [17], PANI at 351 and 429 nm [18], silver nanoparticles at 401 and 429 nm [19] and RGO/PANI/Ag nanocomposite at 260, 350, 400 and 430 nm. The peak at 260 nm represents RGO, peak at 350 nm indicates presence of PANI, peak at 400 nm indicates Ag NPs and peak at 430 nm is a merged peak represents both PANI and Ag NPs. The purity and phase formation of prepared materials were confirmed with XRD and output is showed in Fig. 2. The characteristic peaks centred at ( $2\theta =$ )  $22.6^\circ$  and  $26^\circ$  were correspondent to lattice (002), d-spacing (3.4 Å) signifies the existence of RGO. The crystalline PANI existence was evident by a weak peak of  $15.2^\circ$  and a strong peak at  $25^\circ$  (d – spacing 7.2 and 3.5 Å) and the full width and half maxima (FWHM,  $\sigma_q$ ) of PANI indicates (001) lattice sites. The intense peaks centred at  $2\theta = 38^\circ, 43.999^\circ, 64.1^\circ, 79.2^\circ$  and  $81.8^\circ$  corresponds to (111), (200), (220), (311) and (222) lattice indices of Ag NPs which is well in agreement with standard JCPDS file (No.: 4-0783) [20-21]. In this nanocomposite, a characteristic peak centred at  $15.2^\circ$  represents presence of PANI, the broad peak at  $22.5^\circ$  to  $25^\circ$  is combined peak of RGO with PANI which indicates PANI is diffused between layers of RGO and the intensity of PANI and RGO is much higher.

A stretching vibration of C-O and C=O at 1001  $cm^{-1}$  and 1721  $cm^{-1}$ , -OH deformation at 1390 and 3449  $cm^{-1}$  (Fig. 3). The absence of graphene's absorption peak in IR spectrum which evident for complete transformation of GO into RGO and contains -COOH, -OH, -C=O and C-O [22]. The quinoid ring band were sensitive with two bands at 1561 and 1596  $cm^{-1}$  C-N+ stretching (adjacent to quinoid) was observed at 1385  $cm^{-1}$ , C-N stretching of quinoid benzenoid rings were observed at 1310  $cm^{-1}$ . The N-H bending bands were observed at 1209  $cm^{-1}$ , 1305  $cm^{-1}$  and 1518  $cm^{-1}$  the asymmetric & symmetric stretching of  $NO_2$  (o-nitroaniline) were observed at 1510 and 1346  $cm^{-1}$  respectively. Few broad bands appeared at 1160–1180  $cm^{-1}$  was related to C-H bending, 1230–1255  $cm^{-1}$  was linked to C-N stretching, 1317–1338  $cm^{-1}$  was correlated to C-N+ stretching, 1470–1490  $cm^{-1}$  was associated to C=N stretching, 1580  $cm^{-1}$  assigned to C=C stretching, 1600–1620  $cm^{-1}$  was due to C-C stretching, 1170  $cm^{-1}$  was referred to Benzenoid-(NH<sup>+</sup>), 1110  $cm^{-1}$  was associated to C-H in-plane bending. The bands at 1145 and 831  $cm^{-1}$  were related to the in-plane and out-plane C-H bending [23-24]. FTIR spectra of Ag nanoparticles exhibited prominent peaks at 2928, 1630, 1515, 1384 and 1045  $cm^{-1}$  [25].

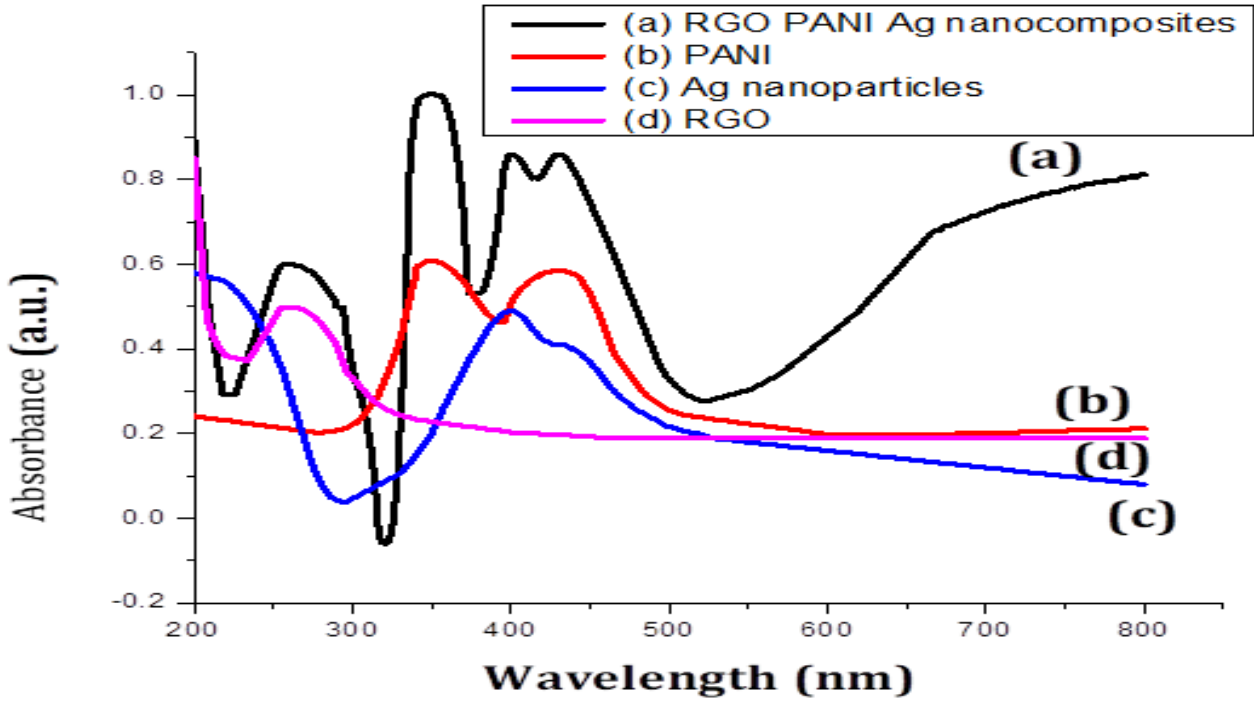


Figure 1. UV-Vis spectra of prepared samples & nanocomposite

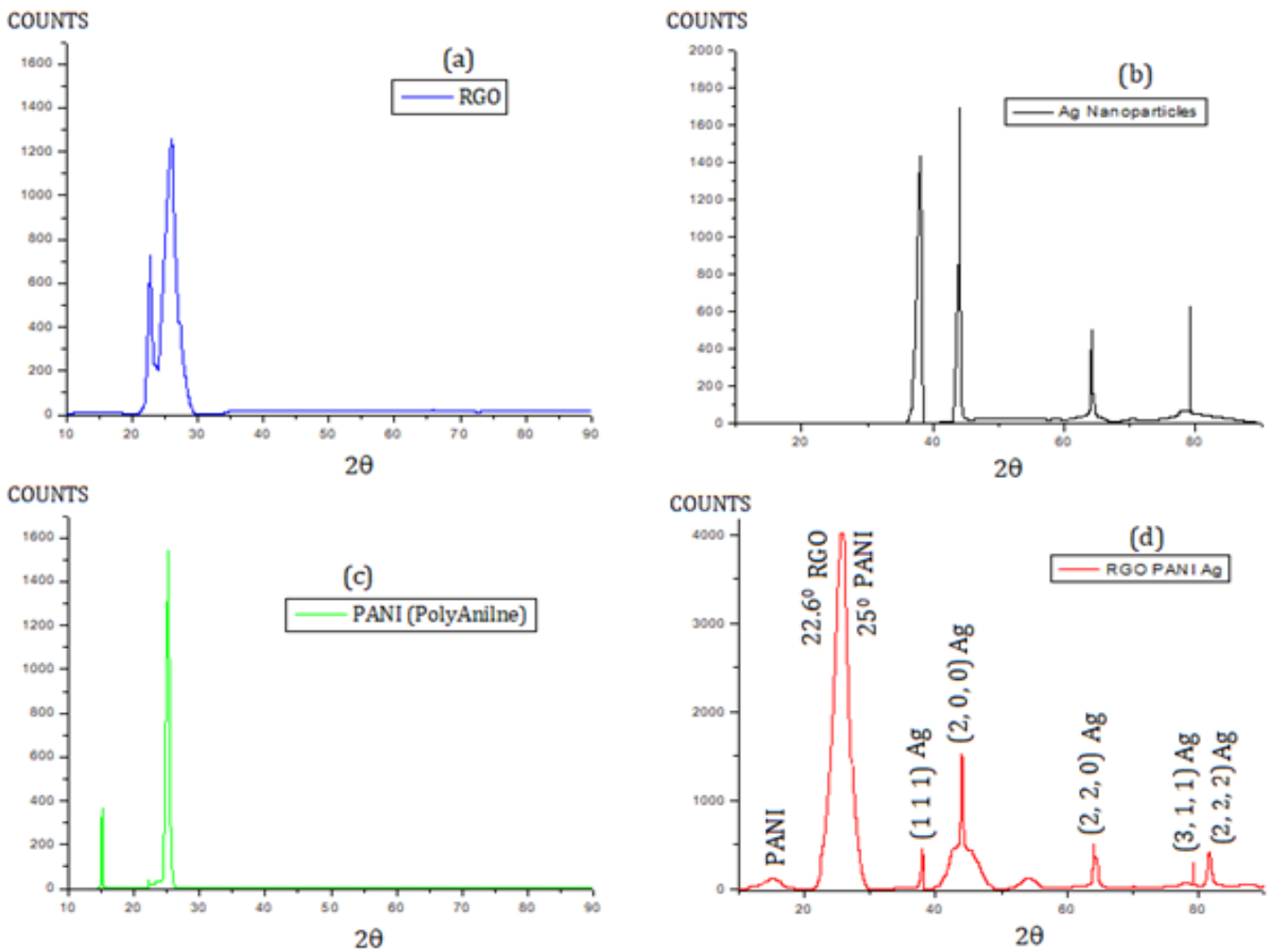


Figure 2. XRD planes of prepared samples and nanocomposite

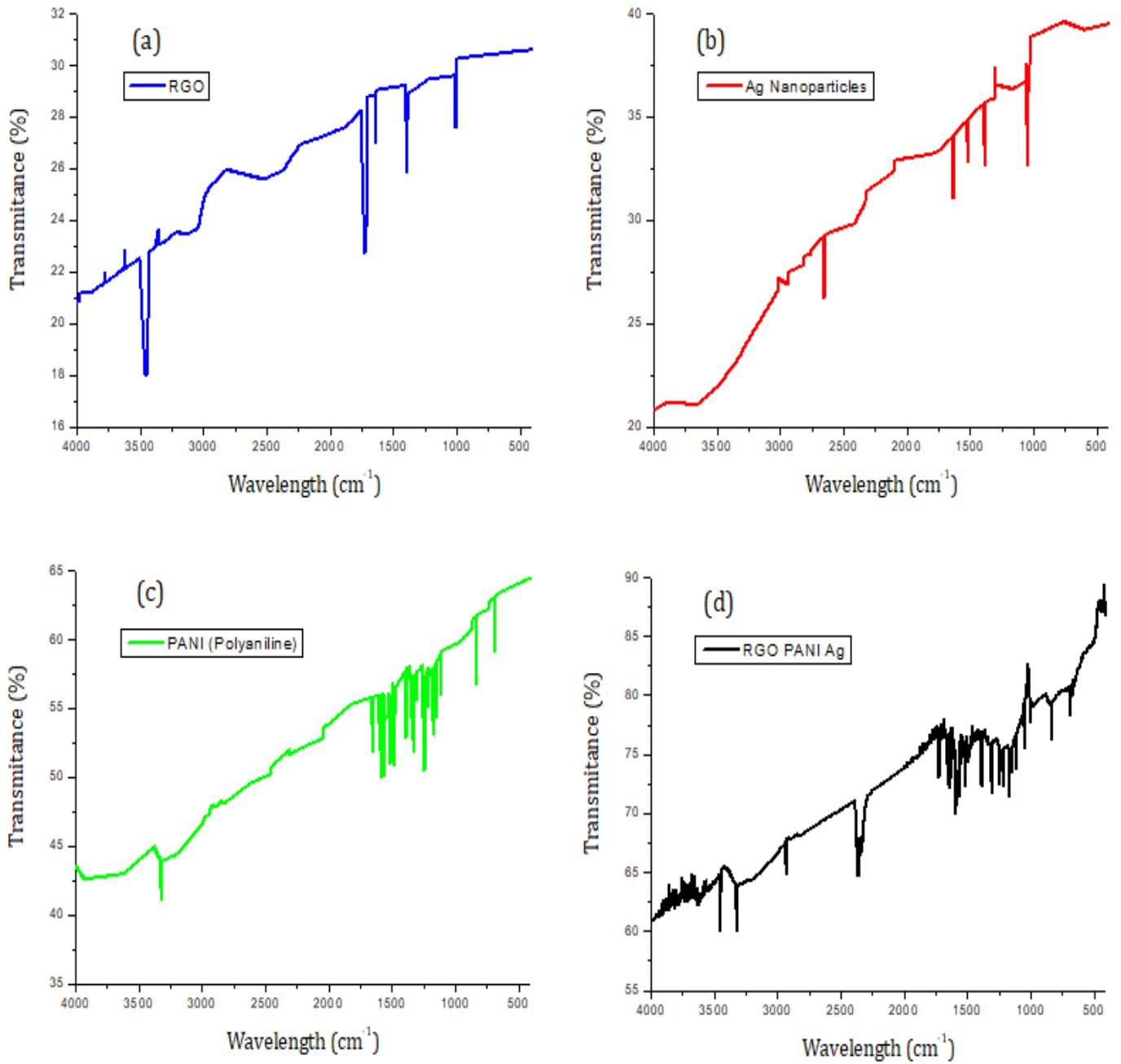
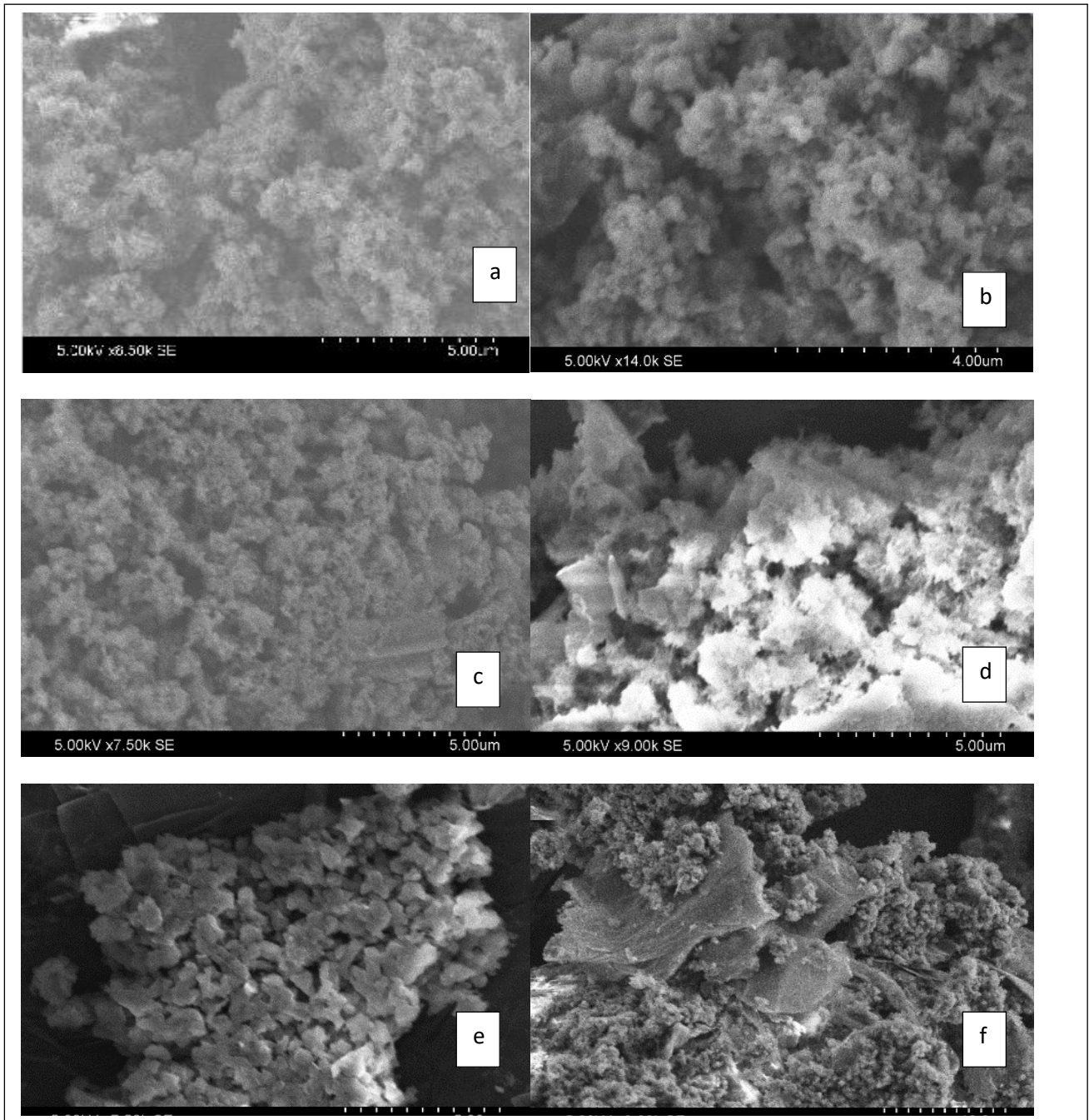
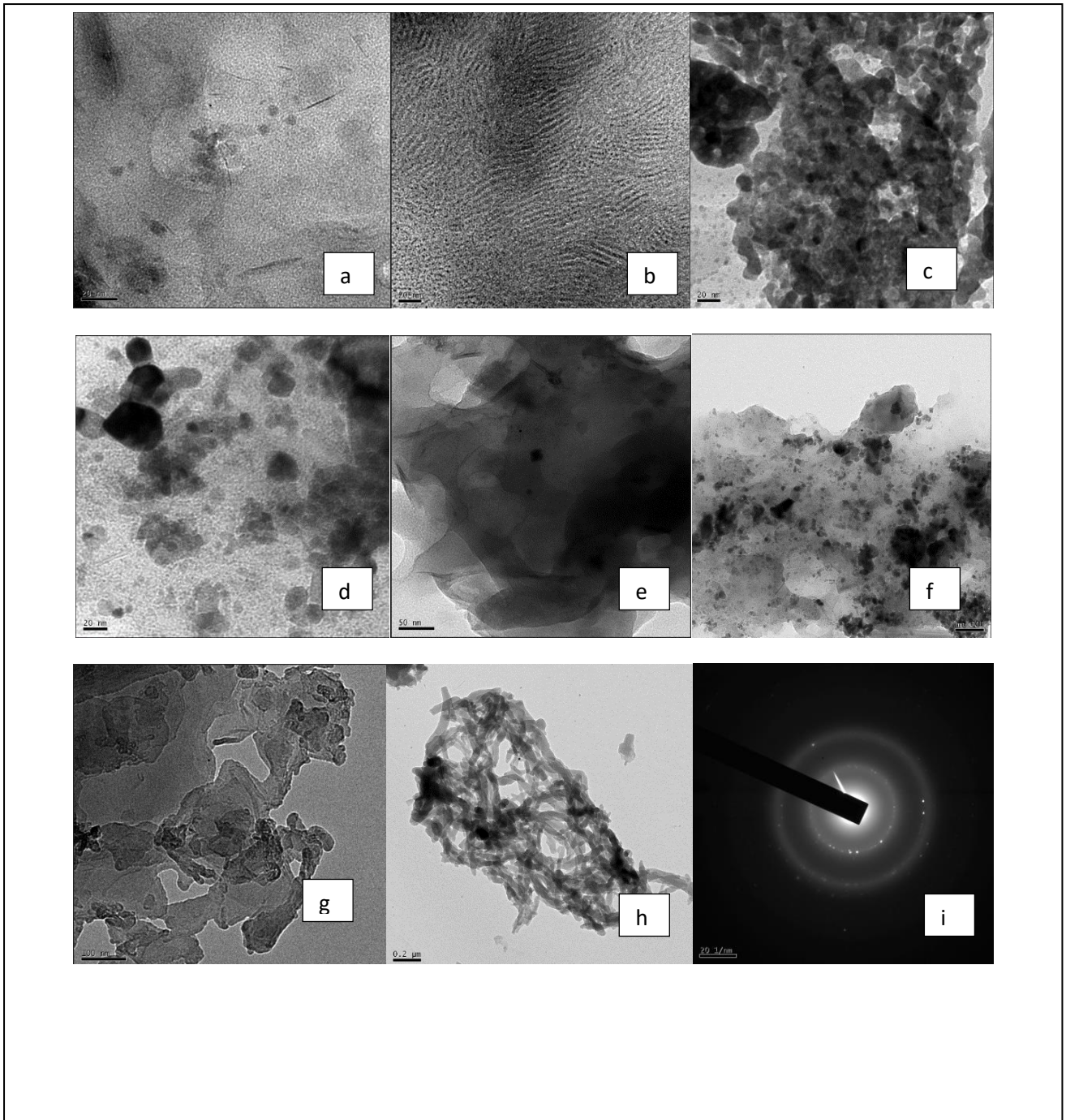


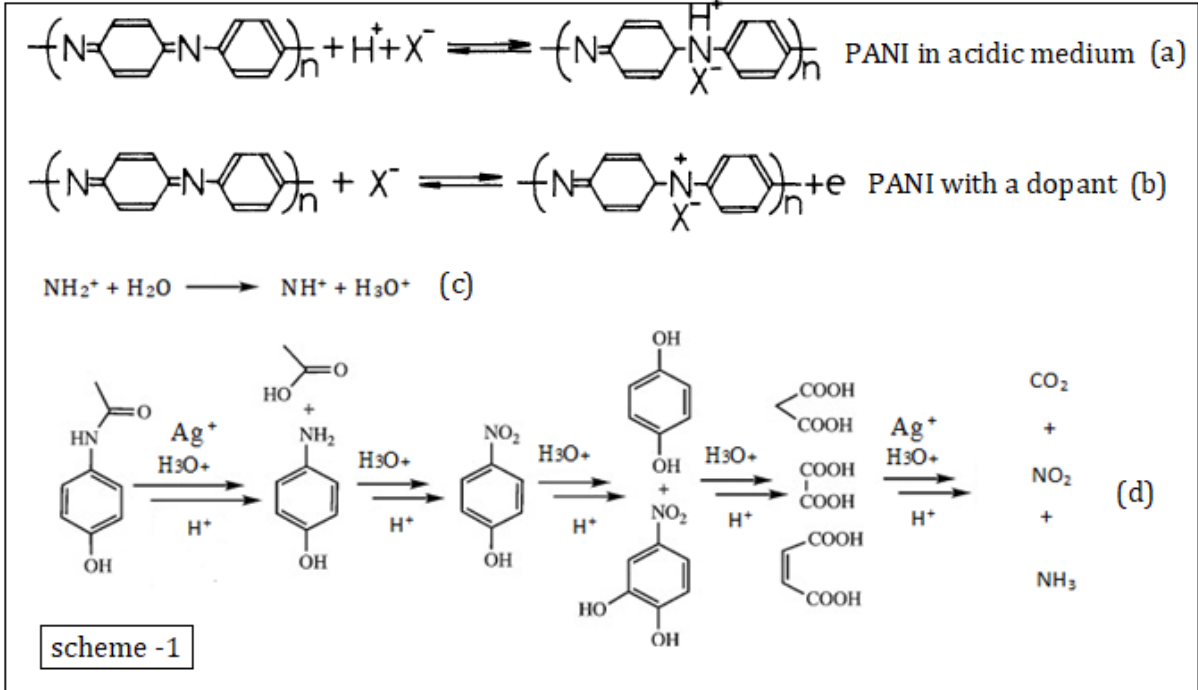
Figure 3. FTIR spectra of prepared samples and nanocomposite



**Figure4.** SEM depicts of prepared a,b) PANI c) PANI with RGO & d-f) RGO/PANI/Ag composite



**Figure 5.** Images of TEM of (a,b) PANI, (c-h) RGO/PANI/Ag nanocomposite and (i) SAED of RGO/PANI/Ag nanocomposite



**Scheme 1.** (a) Indicates formation of imine in PANI in presence of acidic medium, (b) Indicates PANI with dopant Ag nanoparticles, (c) Indicates the formation of Imine and highly reactive Deutonium ion in reaction. (d) Indicates the degradation mechanism of paracetamol with Ag nanoparticles

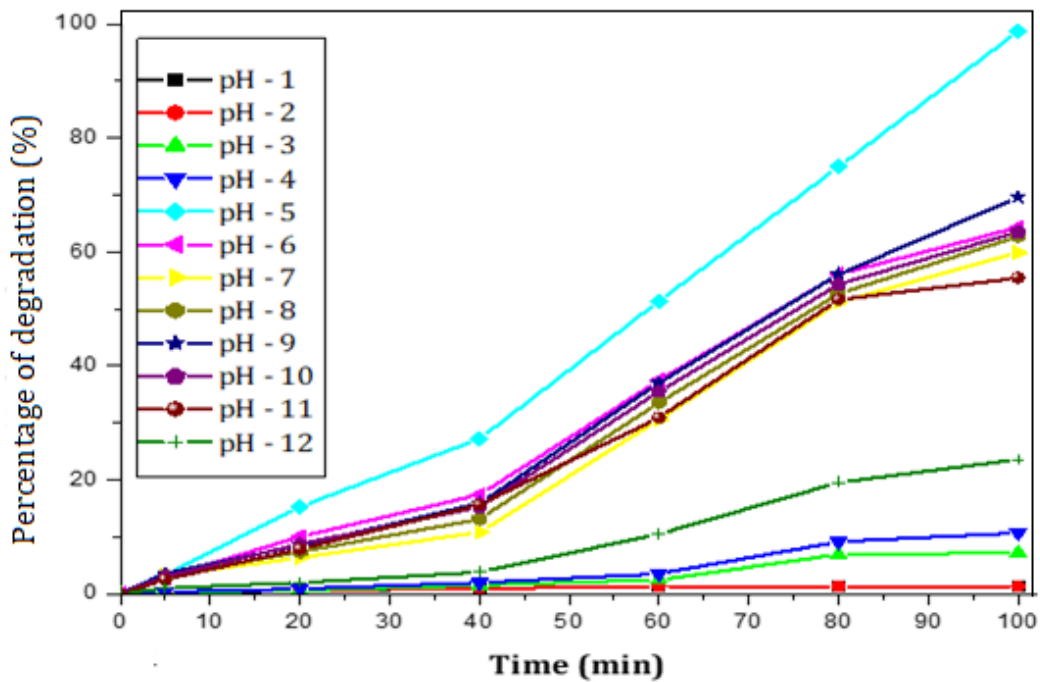


**Figure 6a.**Effect of pH (1 to 12) on Degradation percentage of paracetamol.

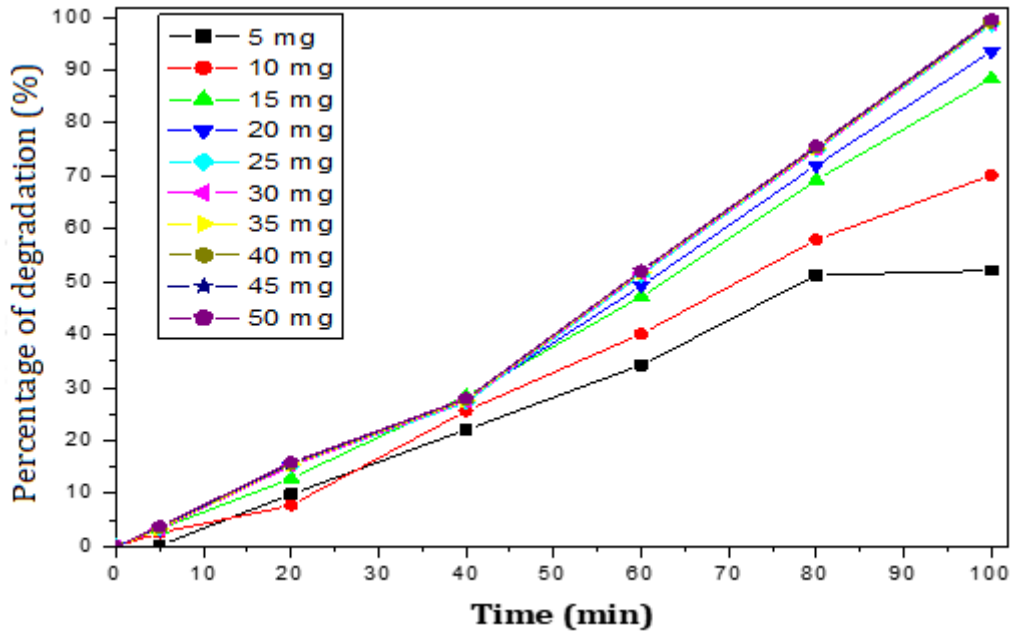


Figure 6b. Paracetamol (pH-5) degradation percentage with variation in composite concentration

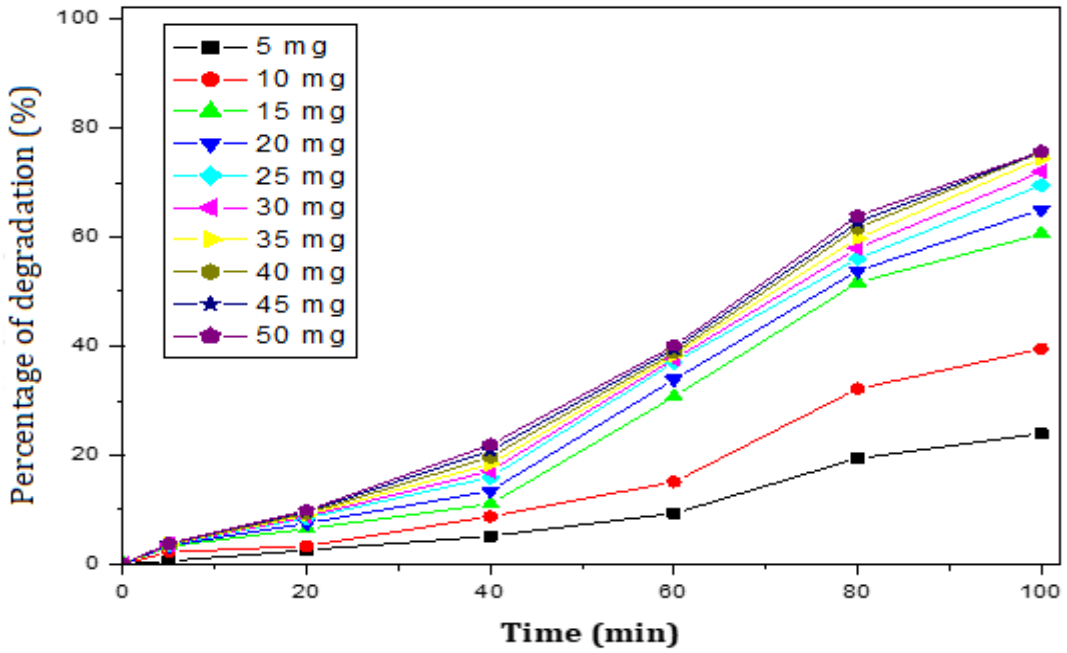
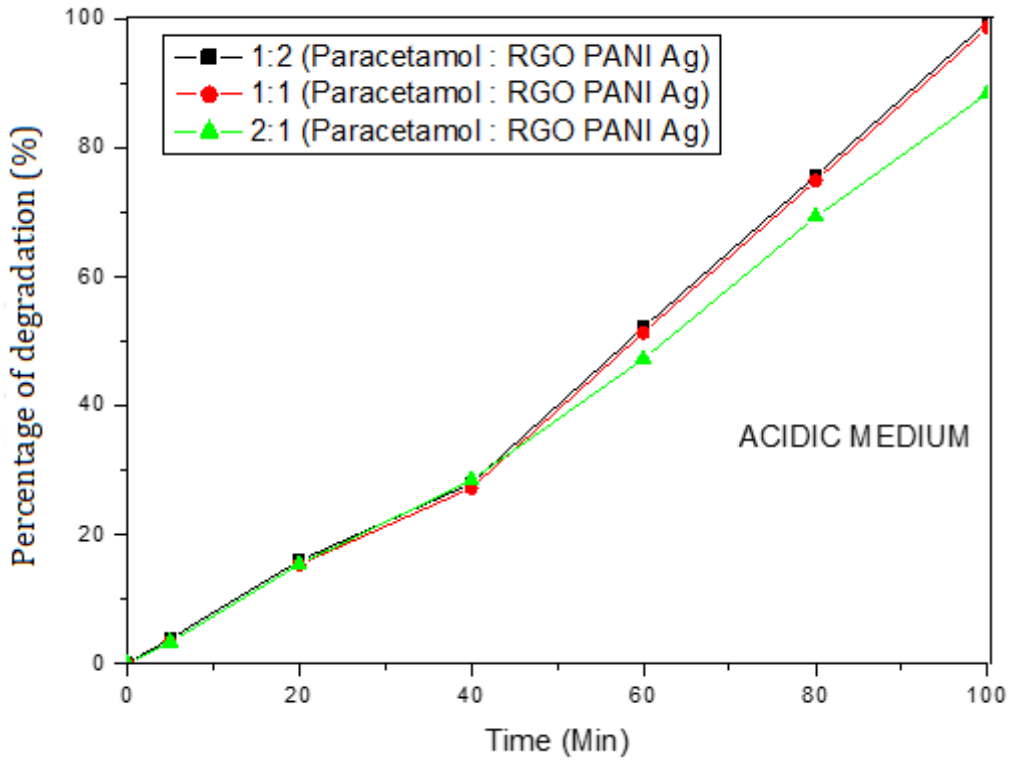
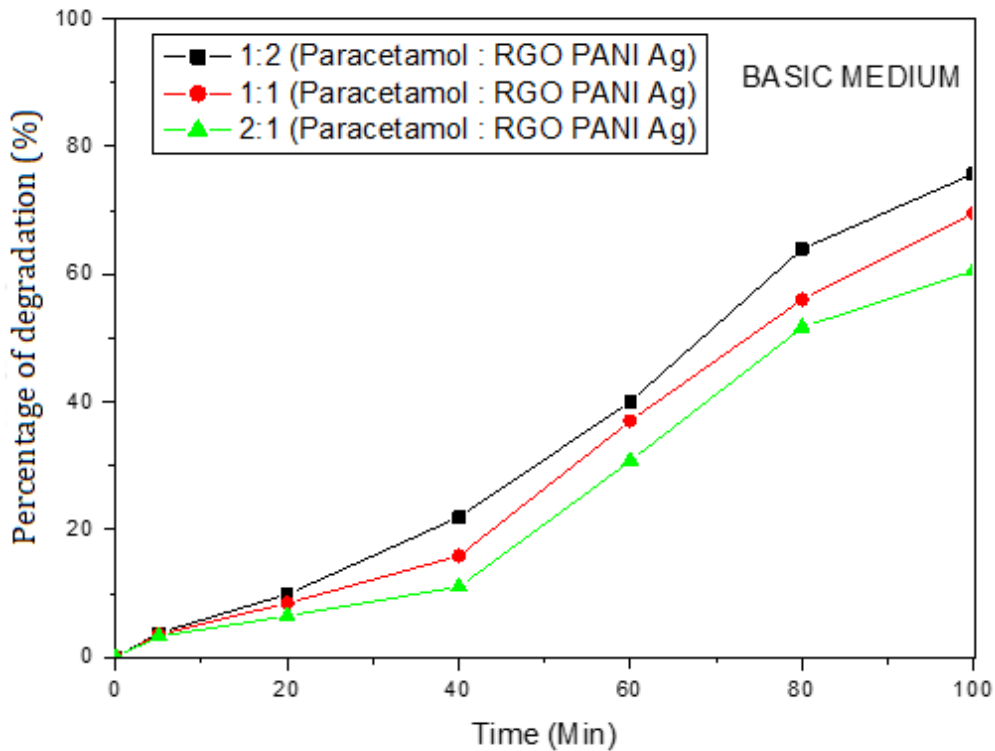


Figure 6c. Paracetamol (pH-9) degradation percentage with variation in composite concentration





**Figure 6d.** Degradation observed by UV-Visible spectrophotometric studies at 245nm in Acidic medium



**Figure 6e.** Degradation observed by UV-Visible spectrophotometric studies at 245nm in Acidic medium

Morphology of prepared composite was investigated SEM and TEM, obtained output is shown in Figures 4&5. The SEM depicts clearly indicate that RGO is the main base of compound and its exfoliation is clearly visible. PANI layer exists over the RGO and the small spherical particles indicate the silver nanoparticles, which were present in between layers of RGO and PANI.

The TEM images clearly indicate the exfoliation of GO and formation of RGO [26]. The sample was studied in range 1µm. The PANI was properly diffused between RGO, It appears like porous membrane on RGO and fine crystals of Ag nanoparticles were amalgamated in it (Figure 5).

**3.2. Photocatalytic degradation of paracetamol using RGO/PANI/Agnanocomposite**

In common, degradation efficiency is greatly relying on size distribution, surface area and composite's functional groups. The RGO/PANI/Ag have shown better degradation of paracetamol, PANI a good conducting material and Silver a good catalyst and anti-microbial individually. The degradation is carried out in constant conditions like normal room temperature and pressure and weight of paracetamol (25 mg), with changes in pH, concentration of composite and in presence of H<sub>2</sub>O<sub>2</sub>.

### 3.2.1. Effect of pH

The deprivation of paracetamol studied at constant conditions and weights of drug and prepared composite is same (25 mg each) with variation in pH from 1 to 12 which is shown in Figure 6a. The degradation is good at pH – 9 and maximum at pH – 5.

### 3.2.2. Concentration of nanocomposites

Paracetamol degradation is subjected with respect to change in prepared nanocomposites' concentration at standard pH (5 & 9) (Fig. 6b & 6c respectively). The paracetamol weight is standard as 25 mg and the composite's weights are 5mg to 50 mg with 5 mg increment. The rate of degradation is good by the nanocomposites (15 mg) and maximum by the nanocomposites (50 mg) which is shown in Figure 6d & 6e.

### 3.2.3. Effect of H<sub>2</sub>O<sub>2</sub>

The H<sub>2</sub>O<sub>2</sub> with different percentages (1%, 2%, so on to 10%) was added to the solution of paracetamol and nanocomposites at constant conditions and equal weights. There is no significant effect on degradation rate of paracetamol as nanocomposites have significantly performed degradation rate (SI).

### 3.2.4. Mechanism

The degradation of Paracetamol at optimum conditions like room temperature, normal pressure, 25 mg of Paracetamol and 50 mg of nanocomposites at pH – 5 and 9 is explained as follows (scheme 1).

### 3.2.5. Acidic medium

In this, RGO acts as binder and support for H<sup>+</sup> and electron transfer. In acidic medium there is no alteration in PANI backbone but there is protonation of amine sites, highly active (good active surface area), it is not easily dissociated in solution but easily transfers protons [27]. The PANI is a good oxidative material, as it becomes protonated emeraldine salt. The –NH chain transfers electrons by converting amine to imine and imine to amine. The excess electrons help in decyclation of aromatic ring structure of paracetamol, this helps in degradation of paracetamol as shown in Fig.6d. This transfer of proton helps paracetamol to converted into hydroquinone and then to benzoquinone. The photolytic degradation of benzoquinone to p-nitrophenol, then to 1,2,4-trihydroxybenzene, then to carboxylic acids, and then to carbon dioxide and minerals was accelerated by silver nanoparticles [28] in acidic medium. The degradation is observed by UV-Visible spectrophotometric studies at 245nm [29].

### 3.2.7. Basic medium

In this RGO acts as binder and support H<sup>+</sup> and electron transfer. In basic medium there is decrease in protonation of amine sites which are highly active, it is not

easily dissociated in solution but rate of transfer of protons is reduced. The PANI is a good oxidative material, as it becomes protonated emeraldine salt, but few H<sup>+</sup> were lost as they form water by combining OH<sup>-</sup> from base. Initially –NH chain transfers electrons by converting amine to imine and vice-versa. The excess electrons help in decyclation of aromatic ring structure of paracetamol, this helps in degradation of paracetamol. This transfer of proton helps paracetamol to converted into hydroquinone to benzoquinone, then to benzoquinone, to p-nitrophenol, then to 1,2,4-trihydroxybenzene, then to carboxylic acids. Here complete mineralisation is prohibited by hydroxyl ions of base but silver nanoparticles act as catalyst and degraded aromatic chain and partial carboxylic acids to minerals [23]. The degradation is observed by UV-Visible spectrophotometric studies at 245nm as presented in Fig.6e [25].

## 4. Conclusion

In this work, a facile synthesis was used for the fabrication of heterostructure composite RGO/PANI/Ag and analyzed by using analytical instruments to study their properties. The paracetamol is subject to photolytic degradation with RGO/PANI/Ag nanocomposites. We found that 99.6% degradation rate of paracetamol in acid nature at optimal conditions are room temperature (300 K), normal pressure, in acidic medium (pH – 5.0) with concentration nanocomposites is 50 mg. In basic medium (pH – 9.0) with same conditions the degradation of paracetamol is 75.76%. In conclude that the proposed composite may be used for degradation of paracetamol in a large scale.

## Funding

No Funding

## Acknowledgment

None

## Conflict of Interest

No conflict of interest

## Author Contribution

All authors are contributed equally.

## References

- [ 1 ] K. Kümmerer, (2008). Pharmaceuticals in the Environment: Sources, Fate and Risks, Springer-Verlag, Berlin, Heidelberg.
- [ 2 ] C. Zwiener, F.H. Frimmel. (2000). Oxidative treatment of pharmaceuticals in water. Water Research. 34: 1881–1885.
- [ 3 ] D.W. Kolpin, E.T. Furlong, M.T. Meyer, E.M. Thurman, S.D. Zaugg, L.B. Barber, H.T. Buxton. (2002). Pharmaceuticals, hormones, and other organics wastewater contaminants in U.S. streams, 1999–2000: a national reconnaissance. Environmental Science and Technology. 36: 1202–1211.
- [ 4 ] K. Pravin, Mutiyara, Sanjay Kumar Gupta, Atul Kumar Mittala (2018). Fate of pharmaceutically active compounds (phacs) from River Yamuna, India: An ecotoxicological risk assessment approach. 150:297– 304.

- [ 5 ] B. Nunes, J. Nunes, A.M.V.M. Soares, E. Figueira, and R. Freitas. (2017). Toxicological effects of paracetamol on the clam *Ruditapes philippinarum*: exposure vs recovery. *Aquatic Toxicology*. 192: 198–206.
- [ 6 ] J.R. Mitchell, S.S.Thorgeirsson, W.Z. Potter, D.J. Jollow, H. Keiser. (1974). Acetaminophen-induced hepatic injury: Protective role of glutathione in man and rationale for therapy. *Clinical Pharmacology & Therapeutics*. 16(4): 676–684.
- [ 7 ] I.A. Donatus, A. Sardjoko, N.P.E. Vermeulen. (1990). Cytotoxic and cytoprotective activities of curcumin. *Biochemical Pharmacology*. 39(12): 1869–1875.
- [ 8 ] P. Moldéus. (1978). Paracetamol metabolism and toxicity in isolated hepatocytes from rat and mouse. *Biochemical Pharmacology*. 27(24): 2859–2863.
- [ 9 ] M.I. Yousef, S.A.M. Omar, M.I. El-Guendi, L.A. Abdelmegid. (2010). Potential protective effects of quercetin and curcumin on paracetamol-induced histological changes, oxidative stress, impaired liver and kidney functions and haematotoxicity in rat. *Food and Chemical Toxicology*. 48(11): 3246–3261.
- [ 10 ] G.S. Sree, S.M.Botsa, B.J.M. Reddy, K.V.B. Ranjitha. (2020). Enhanced UV–Visible triggered photocatalytic degradation of Brilliant green by reduced graphene oxide based NiO and CuO ternary nanocomposite and their antimicrobial activity. *Arabian Journal of Chemistry*. 13 (4): 5137-5150.
- [ 11 ] X. Yang, R.C. Flowers, H.S. Weinberg, and P.C. Singer. (2011). Occurrence and removal of pharmaceuticals and personal care products (ppcps) in an advanced wastewater reclamation plant. *Water Research*. 45(16): 5218–5228.
- [ 12 ] D. Chatterjee, and S. Dasgupta. (2005). Visible light induced photocatalytic degradation of organic pollutants. *Journal of Photochemistry and Photobiology C: Photochemistry Reviews*. 6(2-3): 186–205. doi:10.1016/j.jphotochemrev.2005.09.001
- [ 13 ] S.M.Botsa, K. Basavaiah. (2019). Removal of Nitrophenols from wastewater by monoclinic CuO/RGO nanocomposite. *Nanotechnology for Environmental Engineering*. 4: 1-7.
- [ 14 ] Ravindrakumar G. Bavane, SOPS, NMU, Jalgaon (2014) Synthesis and Characterization of Thin Films of Conducting Polymers for Gas Sensing Applications. 1:1-22.
- [ 15 ] S.M. Botsa, K. Basavaiah. (2020). Fabrication of multifunctional TANI/Cu<sub>2</sub>O/Ag nanocomposite for environmental abatement. *Scientific Reports*. 10: 14080.
- [ 16 ] W.S. Hummers, R.E. Offeman. (1958). Preparation of Graphitic Oxide. *Journal of American Chemical Society*. 80: 1339–1339.
- [ 17 ] S. Gurunathan, J. Woong Han, A. Abdal Daye, V. Eppakayala, and J. Kim. (2012). Oxidative stress-mediated antibacterial activity of graphene oxide and reduced graphene oxide in *Pseudomonas aeruginosa*. *International Journal of Nanomedicine*. 5901.
- [ 18 ] J. Stejskal, P. Kratochvíl, and N. Radhakrishnan. (1993). Polyaniline dispersions 2. UV–Vis absorption spectra. *Synthetic Metals*. 61(3): 225–231
- [ 19 ] N.R. Jana, L. Gearheart, and C.J. Murphy. (2001). Wet chemical synthesis of silver nanorods and nanowires of controllable aspect ratio. *Chemical Communications*. (7): 617–618.
- [ 20 ] S. Park, J. An, J.R. Potts, A.Velamakanni, S. Murali, R.S. Ruoff. (2011). Hydrazine-reduction of graphite- and graphene oxide. *Carbon*. 49(9): 3019–3023.
- [ 21 ] J. Sarkar, D. Chattopadhyay, S. Patra, S.S.Deoa, S. Sinhad, M. Ghosh, A. Mukherjee, K. Acharyaa. (2011). Alternaria Alternata Mediated Synthesis Of Protein Capped Silver Nanoparticles And Their Genotoxic Activity. 563 – 573.
- [ 22 ] K. Gupta, P.C. Jana, and A.K. Meikap. (2010). Optical and electrical transport properties of polyaniline–silver nanocomposite. *Synthetic Metals*. 160(13-14): 1566–1573.
- [ 23 ] D. Ma, X. Li, Y. Guo, and Y. Zeng, (2018). Study on IR Properties of Reduced Graphene Oxide; IOP Conf. Series: Earth and Environmental Science. 108: 022019.
- [ 24 ] A.Dey, S. De, A. De, S.K. De. (2004). Characterization and dielectric properties of polyaniline–TiO<sub>2</sub> nanocomposites. *Nanotechnology*. 15. 1277.
- [ 25 ] Hasik, M.; Drelinkiewicz, A.; Wenda, E.; Paluszkiwicz, C.; Quillard, S. FTIR spectroscopic investigation of polyaniline derivatives-palladium systems. *J. Mol. Struct.* **2001**, 596, 89.
- [ 26 ] P. Devaraj, P. Kumari, C. Aarti, and A. Renganathan. (2013). Synthesis and Characterization of Silver Nanoparticles. *Journal of Nanotechnology*. Article ID 598328, 1-5
- [ 27 ] P. Phanjom, G. Ahmed. (2015). Biosynthesis of Silver Nanoparticles by *Aspergillus oryzae* (MTCC No. 1846) and its Characterizations. *Nanoscience and Nanotechnology*. 5(1): 14-21.
- [ 28 ] L. Stobinski, B. Lesiak, A. Malolepszy, M. Mazurkiewicz, B. Mierzwa, J. Zemek, I. Bieloshapka. (2014). Graphene oxide and reduced graphene oxide studied by the XRD, TEM and electron spectroscopy methods. *Journal of Electron Spectroscopy and Related Phenomena*. 195: 145–154.
- [ 29 ] A. Kitani, J. Izumi, J. Yano, Y. Hiromoto, and K. Sasaki. (1984). Basic Behaviors and Properties of the Electrodeposited Polyaniline. *Bulletin of the Chemical Society of Japan*. 57(8): 2254–2257.